The Effect of Stress Ratio on Fatigue Cracks Growth Rate in Aluminum Alloy

EMAD TOMA KARASH
Northern Technical University/ Technical Institute Mosul, IRAQ

Abstract: - The financial and societal consequences of the sudden failure of various mechanical structures and components can occasionally be severe. As a result, there has been extensive research done on fatigue failure in both the scientific and industrial fields. The impact of stress ratio adjustments on the rates of fatigue fracture propagation for an aluminum alloy has been investigated in the current study. This aluminum alloy was extracted from a Russian MI25 helicopter's primary blade. The stress intensity factor was calculated and employed by creating an initial crack in the test specimens after a specimen of MI25 blade was cut into testing specimens with standard dimensions.

A special program was written specifically for this purpose to draw a graph of the stress intensity factor range (Δk) with value of the propagation of fatigue cracks (da / dN) at each stress ratio (R); Propagation of fatigue cracks has been studied. Finally, the relationship between the two different stress ratios has been discovered. Between the two, a comparison has been established. The findings indicated that when the stress ratio rises, so too does the rate at which fatigue cracks form. Conversely, with a negative stress ratio, the negative increase leads to a reduction in the rate at which fatigue cracks grow. The data have been examined, and during the second stage of crack propagation, where (R = 0.0), pertinent equations that are compatible with the Paris equation have been discovered.

Keywords: - Applied Mechanics, Stress Ration, Fatigue, Fatigue Cracks, Alloys
Received: December 26, 2021. Revised: November 8, 2022. Accepted: December 5, 2022. Published: December 31, 2022.

1. Introduction

One of the principal reasons of failure, particularly in rotating axles, springs, connecting rods, aircraft wings, etc., is vehicle fatigue cracking. This phenomenon is known as fatigue and it occurs because the engineering material is exposed to reciprocating or periodic stresses that are much lower than the material's tensile resistance. The majority of failures of engineering parts occur at stress levels well below the maximum design stress limit, at points where it has a high stress concentration, or when its operational life is increased. When the critical stress density coefficient grows and failure occurs, it includes the growth of tiny cracks in the form of microscopic cracks. Failure fatigue happens when a material's elastic limits are exceeded and the stress changes are below the material's tensile strength. The increase in slit length per cycle (da/dN), which is proportional to the amplitude of the stress intensity component (Δk) during the cycle, is used to define the fatigue growth rate. Given the significance of this subject, extensive study has been done on it recently and is still being done, but despite this, we continue to hear of tragic incidents, the primary cause of which is weariness [1], [2]. The life of the investigated feather is estimated with a restricted time of 1,000 hours in the case of flight or seven years in the case of non-flight in order to work for a limited time. A tire life for a certain number of cycles (N), where the compounds composed of aluminum, copper, etc. are depicted in this type of diagram for nonferrous metal models. They are made for a specific lifespan, but ferrous metal models (Ferro) show the limits of fatigue under lower stress because iron can withstand an infinite number of cycles before failing. There is enough proof that many engineering constructions have pre-existing flaws that develop during manufacturing or piping, thus conjecture starts with the initiation and growth of fatigue from these flaws in the metals used to make automobile and aircraft hulls [3], [4],[5]. Due to its significance in defining the lifetime necessary for these devices, the growth of the crack in a location where the value of (Δk) is low is extremely necessary, making this region the most controlling for determining the amount of fatigue life that concerns aircraft [6],[7]. Numerous studies have focused on the development of fatigue cracking in aluminum alloys used to make aviation vehicles at various frequencies and

temperatures [8], [9], [10]. The effect of the stress strength coefficient ($R = 0.1, 0.3, 0.5$) of an aluminum ingot that is identical to the type (AA- AA- 6063T832) of aluminum ingot used in the production of (MI25) helicopter blades on the development of fatigue fractures. [11],[12],[13] investigated the rate of FCG on intermetallic TiAl at low and high temperatures. Three different Rs were used to set the increased temperature at 750 °C. It was discovered that lowering fatigue thresholds and raising FCG rates are both caused by increasing the stress ratio (R ratio). Additionally, a study on the impact of the tiny FCG strain ratio in Ti-6Al-4V was carried out by [14],[15],[16],[17]. As a result, when the strain ratio is plotted with the slit size function, the effect of R is observed on the tiny slit growth rate, but it has essentially little effect when plotted with the K function. [18] investigated the behavior of crack growth by testing typical CT specimens made of 2024-T4 aluminum alloy under loading in the first mode with various R ratios and crack tips, and discovered that the stress intensity factor was responsible for the increase in FCG rates with rising R ratios. Research in this area is ongoing and not just experiments. There have been several successful simulation research series. In a recent analysis using overloading and simulated plane spectrum loading (mini-Falstaff+), [19] FCG was examined. [20] They studied the beginning and progression of stress cracks in 16MnR steel. The study of the mechanical characteristics of aluminum alloys has been the subject of extensive research [21],[22],[23],[24],[25],[26],[27]. Other models that have been created thus far include [28], [29], [30], [31], [32]. However, the complete models created do not account for the influence of all parameters simultaneously and are not relevant to all materials [28], [29], [30], [31], [32]. In order to understand the fatigue crack growth at various stress ratios and compare them, we will analyze the fatigue crack growth of the aluminum alloy (AA- AA-6063T832) used to make helicopter wings in this article.

2. Materials and working methods

All studies used metal obtained from a helicopter type (MI25) blade, and Figure (1) shows parts in the main tested blade (Main Blade). Figure (3) shows the model's dimensions, which were (5 * 20 * 150) mm, and shows that the model was cut into the necessary number of pieces. On the width of the model, a scratch (slit) was formed with a depth of (0.5) mm and a thickness of (0.2) mm. With the help of these scratches, a sufficient stress intensity was created in the area of highest curvature to mimic real-world conditions. According to its chemical make-up and mechanical characteristics, the metal is an aluminum alloy type (AA- 6063T832). The alloy was examined, and Table provides information on the chemical makeup of the alloy (1). A reputable source was used to determine the alloy's mechanical characteristics [5]. Table provides information on this alloy's mechanical characteristics (2). Moreover, Figure (2) shows models of the main blades of destroyed helicopters, showing the locations and shape of the crack,its growth and collapse of the main blade. Table (1) shows the chemical composition of the aluminum alloy used in the test. Lastly, Table (2) shows the mechanical properties of (6063-T832) aluminum alloy and that of the tested aluminum alloy.

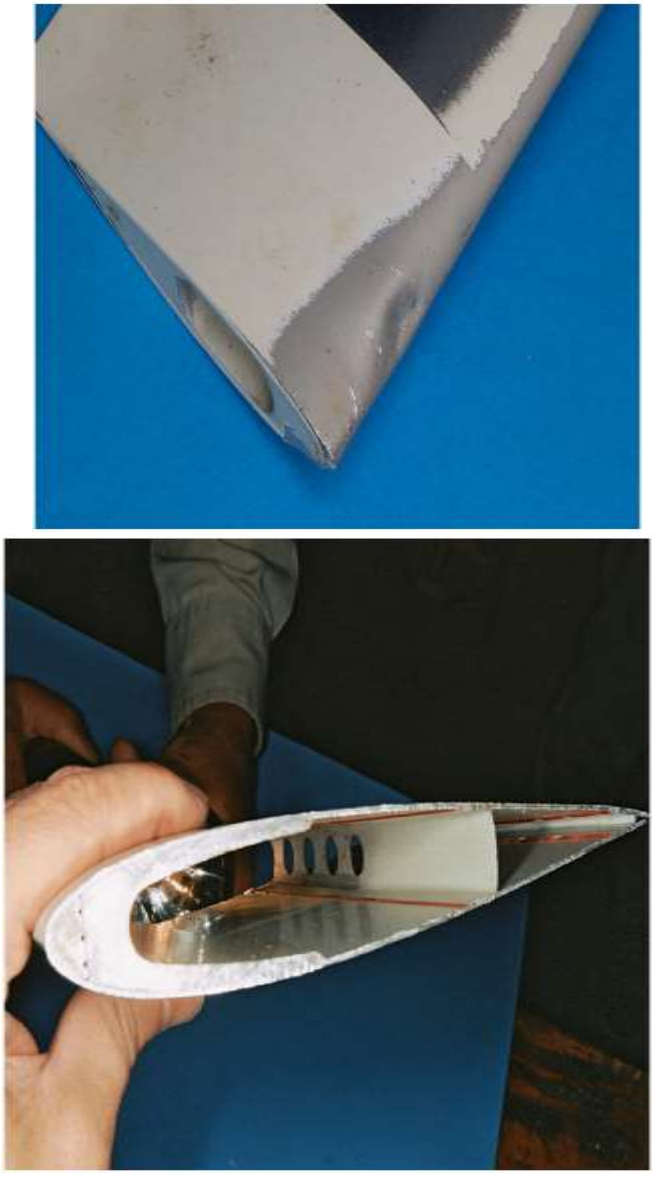

Figure (1) shows sections of the main blade of the helicopter on which the test was conducted

Figure (2) shows models of the main blades of destroyed helicopters, showing the locations and shape of the crack, its growth and collapse of the main blade

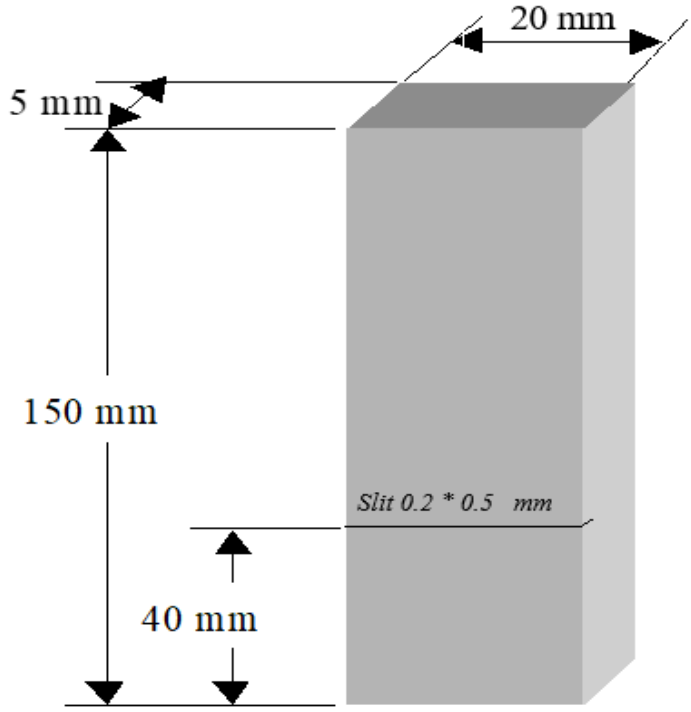

Figure (3) shows the dimensions of the model used in the test

Table (1) shows the chemical composition of the aluminum alloy used in the test

Elements Materials	Zn %	Si %	Fe %	Cu %	Mn %	Mg %	Cr %	Ti %	Al %
Nominal value AA- 6063T832[33]	**0.21 - 0.25**	**0.30 - 0.6**	**0. 1 - 0.35**	**≤ 0.1**	**≤ 0.1**	**0.35 - 0.6**	**≤ 0.05**	**0.13 - 0.25**	**Rem.**
Actual value AA- 6063T832	0.22	0.31	0.32	0.2	0.09	0.53	0.09	0.15	98.09

Table (2) shows the mechanical properties of (6063-T832) aluminum alloy and that of the tested aluminum alloy

Aluminum Alloy	Density, Kg/m^3	Tensile Yield Strength, MPa	Ultimate Tensile Strength MPa	% EL	Modulus of Elasticity, GPa	Shear modulus, Gpa	Hardness (HBW), typical value	Passion's ratio, μ
Nominal value AA- 6063T832 [33]	**2780**	**≥ 160**	**≥ 215**	**≥ 10**	**70**	**28**	**70**	**0.33**
Actual value AA- 6063T832	2750	150	200	9	69	28	68	0.31

The reverse bending machine was used in the test. A mobile optical microscope with a numbered lens (ocular lens) was used in this research, through which the formation and growth of the fissure was observed.
The stress intensity coefficient (ΔK) used to define the stress level was:

$$\Delta K = (\sigma_{max} \quad \sigma_{min}) \sqrt{\pi a}\ F(a/b) \quad (1)$$

Where:

$\Delta K = (stress\ intensity\ factor\ range)$; $a = initial\ crack\ length$;

$\sigma_{max} = (Max.stress\ applied)$; $b = specimen\ thickness$;

$\sigma_{min} = (Min.stress\ applied)$; $F\left(\frac{a}{b}\right) = geometry\ factor.$

$F\left(\frac{a}{b}\right)$: *It can be calculated from the following calibration equation*

$$F(a/b) = 1.122 - 1.40(a/b) + 7.33(a/b)^2 - 13.08(a/b)^3 + 14.0(a/b)^4$$

The calibration of the above equation was given by scientists (Bueckher1960), (Gross1965), (emery,1969), (Benther,1972) and accuracy (0.2%) when the value of (a/b) is equal to or less than (0.6), meaning that (a/b≤0.6 [3] . All tests were carried out in the laboratory atmosphere and at room temperatures around (25°C) and the tests were conducted at a frequency of (5 Hz). As for the slit length measurements, they were calculated using a mobile light microscope with a magnification power (25X-50X) and using a numbered eyepiece installed on the light microscope used in the test along the fissure growth area, where at each stress ratio of the ratios used, which was ($R = -1$,0.0,0.1,0.3,0.5) The model is polished and its surface smoothed well before use, and then the polished surface is divided by clear signs using a vernier caliper on the model with a distance of (0.5) mm between one scratch and another scratch by recording the number of cycles Necessary for the access of the slot to each visa in order to find the relationship between the length of the slot and the number of courses [9], [10].

3. Results and discussion

3-1. First-mode fissure growth

The optical method was used to discover and monitor the growth of the fissure, as a mobile optical microscope was used. The crack growth was monitored on the side where the crack begins to grow, and in calculating the value of the range of stress coefficient for the first phase, equation No. (1) given by Tada (1973) was used. Before conducting the test, the model was polished in the area where the crack is expected to develop, with a good polishing and smoothing of the surface, in order to facilitate the reading process. The surface in which the crack is expected to appear is indicated by means of a vernier with a distance of (0.5 mm) between one visa and another visa. The number of cycles is recorded when the length of the incision reaches to a specified distance by means of a counter on the device and is recorded each time the number of revolutions (Nc) with the length of the slit (a) and until the complete collapse of the model. Figure (4) shows a comparison between the slit length with the number of cycles for the different stress ratios ($R = 0,0.1,0.3,0.5, -1$) when the stress intensity coefficient range value was (ΔK=5.25 MPa). From the figure, we notice that the rate of collapse of the model increases with the increase in the stress ratio, that is, the number of cycles required for the collapse of the model decreases with the increase in the stress ratio at the same stress intensity coefficient (ΔK).

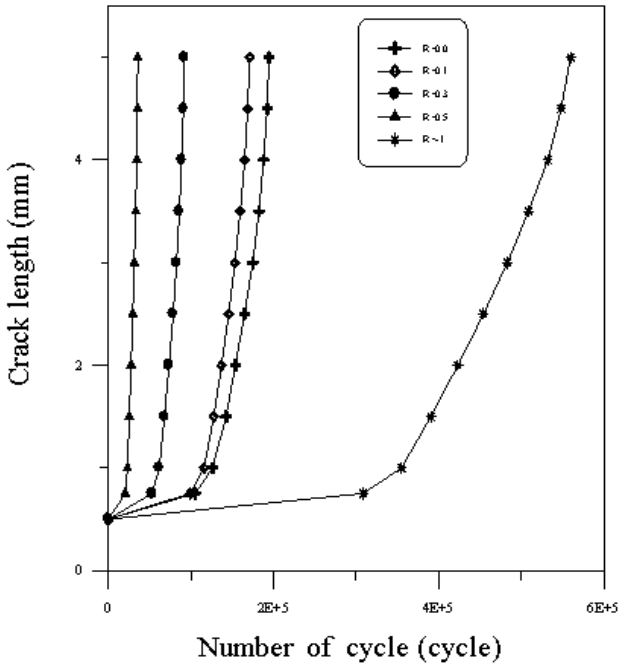

Figure (4) Comparison of the fatigue crack growth curves at different stress ratios

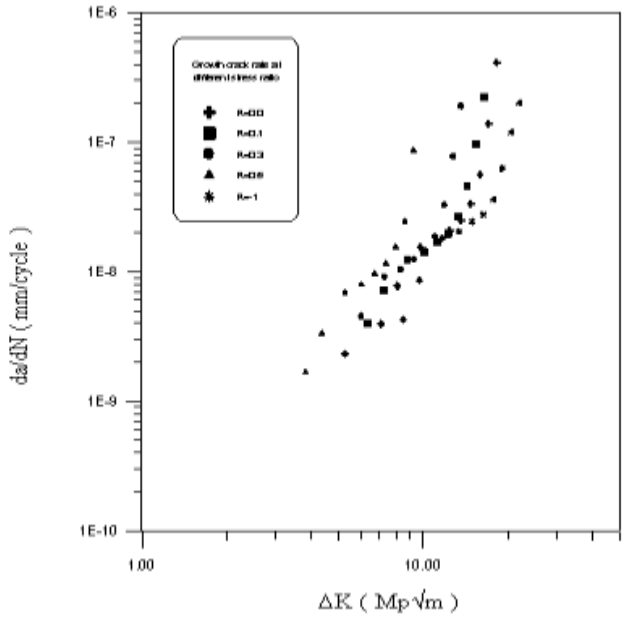

Figure (5) A comparison between the fatigue crack growth rate data for different stress ratios for an aluminum alloy type (AA- 6063T832)

The above results were analyzed by entering a special program. In order to obtain values for the fatigue cracking growth rate (da/dN) with the range values of the stress strength modulus (ΔK) and calibration equation (1) was used in the program to obtain the values of the strain intensity modulus range (ΔK), while the (Finite difference) method was used to obtain the values of Fatigue crack growth rate (da/dN). For the first point, the (Forward difference) method was used, while for the other points, except for the last point, the (Central difference) method was used, and the last point was obtained by the (Backward difference) method.

Through this program, values for the range of stress intensity coefficient (ΔK) were obtained with values for the fatigue crack growth rate (da/dN). Figure (5) illustrates a comparison between the test results. We note from the figure that the positive increase in the stress ratio (R) leads to an increase in the fatigue crack growth rate, while at the stress ratio (R = -1) the value of the fatigue crack growth rate has decreased. Therefore, it can be said that the increase Negative stress ratio leads to a decrease in fatigue crack growth rate.

The effect of the stress ratio on the growth of the fatigue crack can be seen from Figure (6). When the values of the stress ratios are positive, the positive increase in the stress ratios (R) leads to an increase in the growth rate of the fatigue cracking as well. The rate of fatigue crack growth at ($R = 0$) stress increases from (0.0 - 2.2 * 10^{-4} mm/ cycle). At the strain ratio ($R = 0.1$), the fatigue crack growth rate increases from (0.0 - 2.4 * 10-4 mm/cycle), while at the strain ratio ($R = 0.3$) it increases from (0.0 - 4.3 * 10^{-4} mm/cycle)) As for the stress ratio (R = 0.5), the fatigue crack growth rate increases from (0.0 - 1.3 * 10^{-3} mm/cycle), and all models were tested at the same stress intensity factor (Δk = 5.25 Mpa). The positive increase in the stress ratio from ($R = 0.0 - 0.5$) the fatigue crack growth equations also increase from (0.0 - 2.2 * 10^{-4} mm/ cycle) at the stress ratio (R = 0.0) to (0.0 - 1.3 * 10-3). mm/cycle) at a stress ratio ($R = 0.5$), but at a stress ratio ($R = -1$), the crack growth velocity increased from (0.0 - 1.8 * 10^{-4} mm/cycle), and therefore it can be said that the negative increase in the stress ratio Lead to a decrease in the growth rate of fatigue cracking.

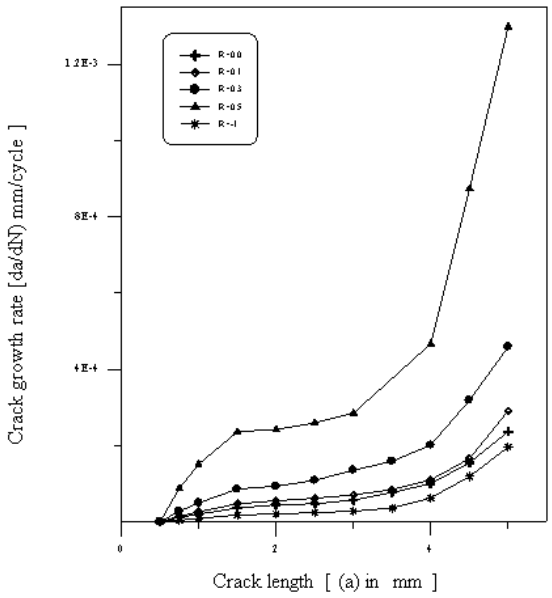

Figure (6) Comparison of fatigue crack growth rate with crack length for different stress ratios

3-2. Effect of the stress ratio on the crack growth rate in the linear region

Early on, the researchers (Lindley & Richards) believed that the crack growth rate in the linear region is relatively sensitive to the effect of the stress ratio (R). In this study, the (Paris) equation was deduced in the linear part of the fatigue crack growth rate for many models at different stress rates [10].

All tests were for prototype slit models. Figure (7) shows the real origin of these equations, which were extracted using a special program called (Curve Export). Figure (8) shows the practical test results and their comparison with (Paris) equation in the second formation stage, the linear stage. Figure (9) shows the results of the tests The different process of stress ratios ($R = 0.0,0.1,0.3,0.5,-1$) and its comparison with (Paris) equation and through the above figures it is clear that an increase in the growth rates of fatigue cracking with the increase of the stress ratio and many previous works confirm an increase in the growth rates of fatigue cracking Increasing the positive stress ratio as the work of researchers (Moddox), (Pearson), (James), (Frost), (March & Pook) and (Nishioka) and others. The increase in crack growth rates is due to an increase in (K_{max}) as it approaches the value of (K_{ic}) for the metal, as well as an increase in the stress rate as well as a decrease in the crack closing effect when the stress ratio increases.

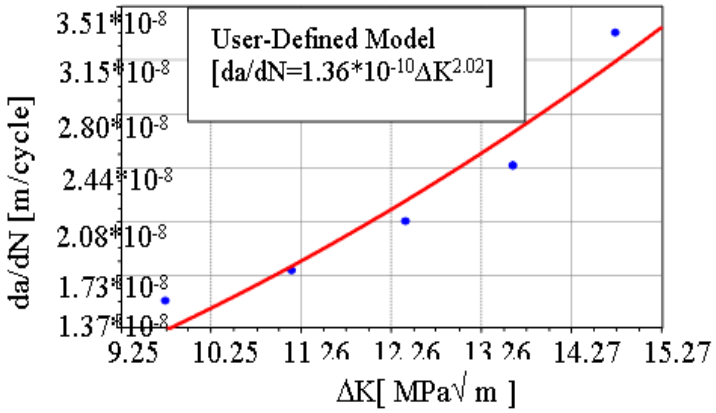

Figure (7) shows how to derive the fatigue crack growth equation for the first phase when (R = 0.0)

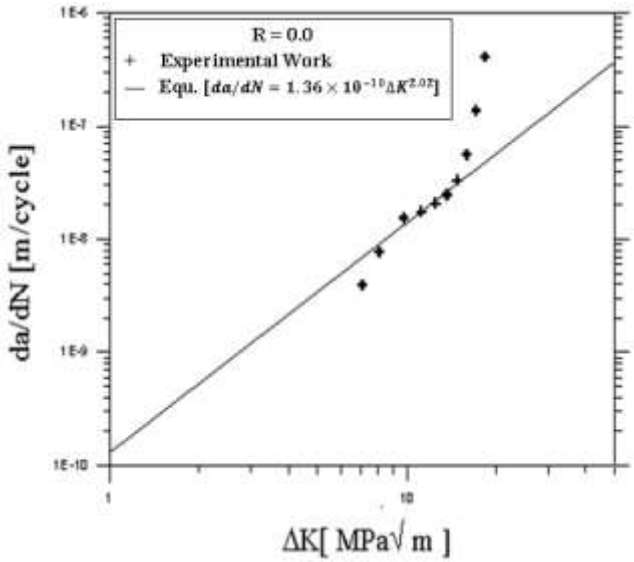

Figure (8) comparing the fatigue crack growth rate with (Paris) equation at stress ratio (R = 0.0).

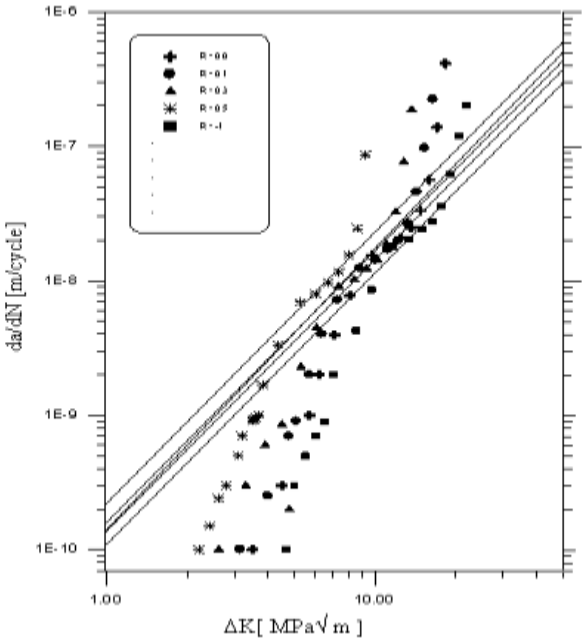

Figure (9) is the growth rate of fatigue cracking in models with an initial crack at different stress ratios in the phase-first tests

The Paris equation for the linear region of fatigue crack growth for the first phase was given as follows:

$$\frac{da}{dN} = C\Delta K^{m} \qquad (2)$$

Were,

ΔK : $(stress\ intensity\ factor\ range)$
N : $number\ of\ cycle$
a : $crack\ length$
$c\ \&\ m$: $pairs\ constant\ equation$

Figure (6) shows a drawing of this equation for a model with an initial slit. In this section, the curve of the fatigue crack growth rate (da/dN) against the full range of the stress intensity modulus (ΔK) will be taken, and it was considered that the lowest rate of fatigue cracking growth rate at the beginning of the fatigue cracking (Threshold) is ($1*10^{-10}$ m/cycle).

The practical values were taken from the value of (ΔKth) and the values of the fatigue crack growth rate in the first and second stages to the last point in the linear region of the fatigue crack growth and at a stress ratio (R = 0.0), which is in similar behavior at different stress ratios because the effect of stress ratios (R) In the linear phase of slightly fatigue crack growth. The following equation has been considered:

$$\frac{da}{dN} = C\Delta K^{m} - D \qquad (3)$$

This equation was taken to represent the fatigue crack growth behavior for the first and second stages, and (Curve Expert) program was used to derive the values of the constants. The following equation was obtained:

$$\frac{da}{dN} = 0.144*10^{-9}\,\Delta K^{2.02} - 1.714*10^{-9} \qquad (4)$$

This equation describes the growth of fatigue cracking in the first and second stages, i.e., the phase of onset and progression of fatigue and the linear phase of fatigue crack growth, which is consistent with (Paris) equation.

Figure (10) shows a comparison between the fatigue crack growth equation (4) for the first phase with the practical results and the (Paris) equation in the linear region and the (Paris) equation in the linear region are

$$\Delta K_{th} = \Delta k_o$$

The figure shows an acceptable match between the practical and inferred values.

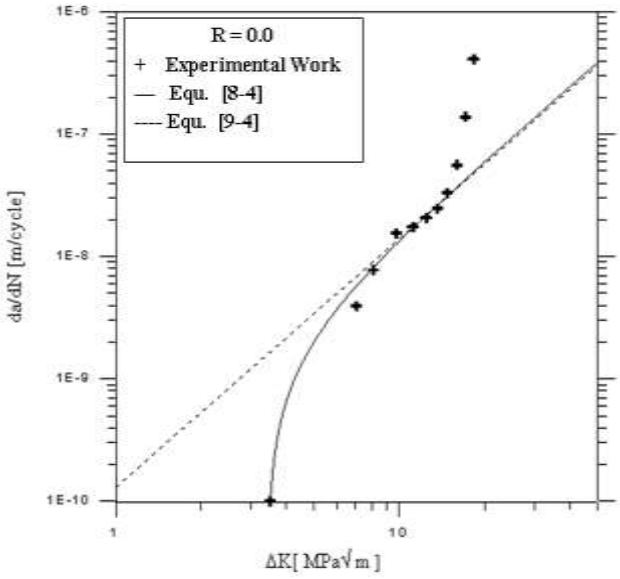

Figure (10) Comparison of the equation for the crack growth rate of the whole for the first phase with the practical results and an equation (Paris)

4. Conclusions

1. To describe the crack growth in the first and second phases of the first phase testing, a new equation for the fatigue crack growth was developed.
2. The results of the fatigue crack growth tests show that the number of cycles required to collapse the model at positive values of the stress ratios (R) reduces as the positive stress ratio (R) increases at the same values of the used stress intensity coefficient (ΔKth). The more negative the stress ratios (R) are, the more cycles must pass until the model collapses.
3. According to the findings of the analysis of fatigue crack growth, the fatigue crack growth rate (Kth) reduces at stress ratios (R = -1), whereas it increases with a positive increase in the stress ratios (R)..

Acknowledgment

This work was supported through Northern Technical University, Iraq. by the Research Program of the Engineering Science, (No. 001233- 2020).

References

[1]. Ashbaugh, N.E., B. Dattaguru, M. Khobaib, T. Nicholas, R.V. Prakash, T.S. Ramamurthy, B.RSeshadri and R. Sunder, 1997. Experimental and Analytical Estimates of Fatigue Crack Closure in an Aluminum-copper Alloy, Fatigue & Fracture engineering Materials & Structures, 20: 963-974.

[2]. Mann,J.Y.,"Fatigue of Materials", an introductory text , London , Melbourne university press : xv , 155 p . (1976) .

[3]. W . Bulton , " Engineering Materials Technology " , Third Edition , Printed and Bound in Great Britain , (1998) .

[4]. Hudson , C.M. & Scardina , J.T .," Effect of Stress Ratio on Fatigue Crack Growth in (7075 – t6) Aluminum – Alloy Sheet " , Engineering Fracture Mech . 1,429-466 (1969) .

[5]. Davis , J.R " Metals Handbook " , Second Edition , Desk Edition , Prepared Under the Direction of the ASM International Handbook Committee , (1998) .

[6]. W . Bulton , " Engineering Materials Technology " , Third Edition , Printed and Bound in Great Britain , (1998) .

[7]. Purushothaman . S ., " Generalized Theory of Fatigue Crack Propagation ", ph . D. Thesis Columbia University , (1976) .

[8]. J. C. Newman Jr., "Analyses of Fatigue Crack Growth and Closure Near Threshold Conditions for Large-Crack Behavior," *Fatigue Crack Growth Thresholds, Endurance Limits, and Design*, ASTM STP 1372, J. C. Newman Jr. and R. S. Piascik, eds., American Society for Testing and Materials, West onshohocken, PA (2000), pp. 227-251.

[9]. Mackay , T . L ., " Fatigue Crack Propagation Rate at Low of Two Aluminum Sheet Alloy 2024 - T3 & 7075 – T5 , Materials and Reducibility Dough's Aircraft Company . Long Beach , CA 90846 , USA , Engineering Fracture Mechanics Volume , 11 , PP . 753 – 761 (1979) .

[10]. Mohammed , R.A. " The Growth Fatigue Cracks in a Turbine Shaft Steel Under Mixed I & II , ph.D. TSU , January (1993) .

[11]. C. C. Rusu, L. R. Mistodie., The Effect Of Stress Ratio On Fatigue Threshold Of Crak In Mode (I), Al-Qadisiyah Journal for Engineering Sciences, 2014, Vol. 7 (4), pp. 187-200.

[12]. J. Zheng and B. E. Powell, Effect of Stress Ratio and Test Methods on Fatigue Crack Growth Rate for Nickel Based Superalloy Udimet720, Int J Fatigue,21 (1999) 507-513

[13]. S. J. Zhu, L. M. Peng, T. Moriya, and Y. Mutoh, Effect of Stress Ratio on Fatigue Crack Growth in Tial Intermetallics at Room and Elevated Temperatures, Mater Sci Eng: A,290 (2000) 198-206

[14]. M. Caton, R. John, W. Porter, and M. Burba, Stress Ratio Effects on Small Fatigue Crack Growth in Ti–6al–4v, Int J Fatigue,38 (2012) 36-45

[15]. G. Yang, Z. L. Gao, F. Xu, and X. G. Wang, An Experiment of Fatigue Crack Growth under Different R-Ratio for 2024-T4 Aluminum Alloy, Appl Mech Mater,66 (2011) 1477-1482

[16]. J. C. Newman Jr, J. W. Shaw, B. S. Annigeri, and B. M. Ziegler, Fatigue and Crack Growth in 7050-T7451 Aluminum Alloy under Constant-and Variable-Amplitude Loading, J. Eng. Gas Turbines Power,135 (2013) 022101-1

[17]. X. Wang, D. Yin, F. Xu, B. Qiu, and Z. Gao, Fatigue Crack Initiation and Growth of 16mnr Steel with Stress Ratio Effects, Int J Fatigue,35 (2012) 10-15

[18]. A. Standard, E647, Standard Test Method for Measurement of Fatigue Crack Growth Rates, Annual Book of ASTM Standards, Section Three: Metals Test Methods and Analytical Procedures,3 (2000) 628-670

[19]. M. C. N. Pugnoa, P. Cornettia, A. Carpinteri, A Generalized Paris' Law for Fatigue Crack Growth, J Mech Phys Solids,54 (2006) 1333–1349

[20]. J. M. C. L.P. Borrego , S. Silva , J.M. Ferreira, Microstructure Dependent Fatigue Crack Growth in Aged Hardened Aluminium Alloys, Int J Fatigue,26 (2004) 1321-1331

[21]. Sandnes L, Grong Ø, Torgersen J, Welo T, Berto F. Exploring the hybrid metal extrusion and bonding process for butt welding of Al–Mg–Si alloys. Int J Adv Manuf Technol. 2018; 98(5):1059-1065.

[22]. Berto F, Sandnes L, Abbatinali F, Grong Ø, Ferro P. Using the hybrid metal extrusion & bonding (HYB) process for dissimilar joining of AA6082-T6 and S355. Procedia Struct Integr. 2018;13: 249-254.

[23]. Blindheim J, Grong Ø, Aakenes UR, Welo T, Steinert M. Hybrid metal extrusion & bonding (HYB)—a new technology for solid-state additive manufacturing of aluminium components. Procedia Manuf. 2018;26:782-789

[24]. E. T. B. Karash, S. R. Yassen, M. T. E. Kassim., Effect of friction stir welding parameters on the impact energy toughness of the 6061-t6 aluminum alloys, Annals of "Dunarea de Jos" University, Fascicle XII ISSN 1221-4639 Welding Equipment and Technology, 2018, Vol. 29, pp. 27-32.

[25]. Emad T. B. K., Saeed R. Y., Mohammed T. E. Q., The Effect of the Cutting Depth of the Tool Friction Stir Process on the Mechanical Properties and Microstructures of Aluminum Alloy 6061-T6, American Journal of Mechanics and Applications 2015; 3(5): pp 33-41.

[26]. Collipriest JE Jr. An Experimentalist's view of the surface flaw problem. physical problems and computational solutions", Swedlow JL Ed, ASME, 43-62, 1972.

[27]. He Y, Shu W, Cui R, Wu L. Total fatigue life prediction under constant amplitude loading. Mater Scie Forum 2012; 704-705: 636-640.

[28]. Abdullah, O.F., Hussein, O.A., Karash, E.T., The laser surface treatment effective on structural properties for invar alloy (Fe-Ni) type prepared by powder technology, Key Engineering Materialsthis link is disabled, 2020, 844, pp. 97–103

[29]. Sultan, J.N., Najem, M.K., Karash, E.T., Effect of heat-treatment temperature on the corrosion behaviour of cold worked 6111 aluminium alloy, Journal of the Korean Society for Precision Engineeringthis link is disabled, 2021, 38(6), pp. 385–395

[30]. Sultan, J.N., Abbas, M.K., Abd-Al Kareem Ibrahim, M., ...Ali, A.M., Ibrhim, H.A., Corrosion Behavior of Thermal Seamless Carbon Steel Boiler Pipes, Annales de Chimie: Science des Materiaux , 2021, 45(5), pp. 399–405

[31]. Sultan, J.N., Karash, E.T., Abdulrazzaq, T.K., Elias Kassim, M.T., The Effect of Multi-Walled Carbon Nanotubes Additives on the Tribological Properties of Austempered AISI 4340 Steel, Journal Europeen des Systemes Automatisesthis link is disabled, 2022, 55(3), pp. 387–396

[32]. He Y, Shu W, Cui R, Wu L. Total fatigue life prediction under constant amplitude loading. Mater Scie Forum 2012; 704-705: 636-640.

[33]. Aluminium 6060 T5, T6, T4; Aluminum Alloy 6060 Properties, https://www.theworldmaterial.com/aluminum-6060/.

Contribution of Individual Authors to the Creation of a Scientific Article (Ghostwriting Policy)

The author(s) contributed in the present research, at all stages from the formulation of the problem to the final findings and solution.

Sources of Funding for Research Presented in a Scientific Article or Scientific Article Itself

This work was supported through Northern Technical University, Iraq. by the Research Program of the Engineering Science, (No. 001233- 2020).

Conflict of Interest

The author(s) declare no potential conflicts of interest concerning the research, authorship, or publication of this article.